

Linear-scaling self-consistent implementation of the van der Waals density functional

Andris Gulans, Martti J. Puska, and Risto M. Nieminen

Department of Applied Physics, COMP, Helsinki University of Technology, P.O. Box 1100, 02015 TKK, Finland

(Received 6 March 2009; revised manuscript received 9 April 2009; published 13 May 2009)

An efficient linear-scaling approach to the van der Waals density functional in electronic-structure calculations is demonstrated. The nonlocal correlation potential needed in self-consistent calculations is derived in a practical form. This enables also an efficient determination of the Hellmann-Feynman forces on atoms. The numerical implementation employs adaptive quadrature grids in real space resulting in a fast and an accurate evaluation of the functional and the potential. The approach is incorporated in the atomic orbital code SIESTA. The application of the method to the S22 set of noncovalently bonded molecules and comparison with the quantum chemistry data reveal an overall agreement but show that different exchange functionals should be used for different types of bonds.

DOI: 10.1103/PhysRevB.79.201105

PACS number(s): 71.15.Mb, 31.15.E–

The van der Waals (vdW) interaction plays an important role in various processes in biochemistry, in surface science, and in physics of layered materials. Although the basic underlying physics of dispersion forces is understood, an accurate and efficient calculation of the vdW interaction is still challenging.

The post-Hartree-Fock approaches, based on perturbation theory, are able to treat the vdW interaction. For instance, the coupled-cluster methods¹ [especially coupled-cluster with single and double and perturbative triple excitations, CCSD(T)] are very accurate and often used in benchmark calculations. Unfortunately, the high precision comes with enormous computational expenses, making the method fully applicable only for small complexes with less than a few dozen of atoms. The second-order Møller-Plesset perturbation theory (MP2), although less expensive and less accurate, also contains the essential physics for describing the vdW interaction. Both of the two methods are not straightforward to apply to extended systems and the existing approaches to periodic systems, as those in Refs. 2 and 3, are fairly expensive and not in common use.

Another class of methods for electronic-structure calculations is based on the density-functional theory (DFT). The standard approximations to the exchange-correlation energy in DFT, such as the local-density approximation (LDA) and the generalized-gradient approximation (GGA), are relatively cheap and easily applicable also to periodic systems. Unfortunately, these methods cannot describe the dispersion interaction properly. The problem has been addressed by Langreth, Lundqvist and co-workers,^{4–6} who constructed a nonlocal correlation functional aiming to preserve the essential mechanisms behind the vdW interaction. This approach has been successfully utilized for selected test systems and applications.^{7–10} However, most of these results are obtained either using an *a posteriori* energy correction scheme or a self-consistent calculation with a restricted capability of relaxing the structures. The reason for this is the computational complexity of the self-consistent approach of Ref. 11, which was employed in the earlier self-consistent calculations.

In this Rapid Communication, we demonstrate our alternative highly efficient real-space approach. We derive the functional derivative of the vdW density functional (vdW-DF) and obtain a representation, which enables a simpler

evaluation of the nonlocal correlation potential and forces for self-consistent calculations with full atomic relaxation. Our implementation employs numerical quadratures on adaptive grids, which vary depending on the local properties of the electron density and are optimized to calculate the vdW-DF. We perform calculations on the widely used molecular benchmark set S22.¹² The results for its molecular complexes provide an extensive test for the reliability of the vdW-DF. Simple examples such as noble gas dimers are not suitable for these purposes as they do not provide a complete picture with respect to the variation in the nature of the bonding. Extended systems are either not discussed as a systematic discussion would require a versatile test set, which does not exist.

Starting from the adiabatic connection-fluctuation dissipation theorem, Dion *et al.*⁴ derived the nonlocal part of the correlation energy in the compact form

$$E_c^{\text{nl}}[n] = \frac{1}{2} \int \int n(\mathbf{r}) \varphi(\mathbf{r}, \mathbf{r}') n(\mathbf{r}') d^3r d^3r', \quad (1)$$

where $n(\mathbf{r})$ is the electron density and $\varphi(\mathbf{r}, \mathbf{r}')$ is a kernel. Following Dion *et al.*,⁴ we write the kernel as a function of the dimensionless variables D and Δ defined as

$$D = \frac{q_0(\mathbf{r}) + q_0(\mathbf{r}')}{2} |\mathbf{r} - \mathbf{r}'|, \quad (2)$$

$$\Delta = \frac{q_0(\mathbf{r}) - q_0(\mathbf{r}')}{q_0(\mathbf{r}) + q_0(\mathbf{r}')}, \quad (3)$$

where $q_0(\mathbf{r})$ is a characteristic wave number, which depends on the density and its gradient at the given point \mathbf{r} . Additionally it can be related to the radius of the sphere, where the kernel function is mostly localized.

For self-consistent calculations, an algorithm to evaluate also the correlation potential is required. One method is introduced in Ref. 11. However, we suggest a different approach. The functional derivative $v_c^{\text{nl}}(\mathbf{r}) = \delta E_c^{\text{nl}} / \delta n(\mathbf{r})$ is evaluated using the variables D and Δ . Employing the chain rule, after straightforward but rather tedious steps, we obtain the expression

$$\begin{aligned}
v_c^{\text{nl}}(\mathbf{r}) = & 2\varepsilon_c^{\text{nl}}(\mathbf{r}) + \frac{1}{2} \left\{ n(\mathbf{r}) \frac{\partial q_0(\mathbf{r})}{\partial n(\mathbf{r})} - \nabla \left[n(\mathbf{r}) \frac{\partial q_0(\mathbf{r})}{\partial \nabla n(\mathbf{r})} \right] \right. \\
& - n(\mathbf{r}) \frac{\partial q_0(\mathbf{r})}{\partial \nabla n(\mathbf{r})} \nabla \left. \int n(\mathbf{r}') \left\{ \frac{\partial \varphi}{\partial D} |\mathbf{r} - \mathbf{r}'| \right. \right. \\
& \left. \left. + \frac{\partial \varphi}{\partial \Delta} [q_0(\mathbf{r}) + q_0(\mathbf{r}')]^2 \right\} d^3 r' \right\}, \quad (4)
\end{aligned}$$

where the energy density is

$$\varepsilon_c^{\text{nl}}(\mathbf{r}) = \frac{1}{2} \int \varphi(\mathbf{r}, \mathbf{r}') n(\mathbf{r}') d^3 r'. \quad (5)$$

Equations (4) and (5) contain only a single integral over \mathbf{r}' , which can be conveniently evaluated numerically in spherical coordinates $\tilde{\mathbf{r}}$ with \mathbf{r} as the origin, i.e., $\tilde{\mathbf{r}} = \mathbf{r}' - \mathbf{r}$. The choice of spherical instead of Cartesian coordinates is inspired by the shape of the kernel function. First, it is localized in space within a radius that can be defined locally. Second, it has a logarithmic singularity at the point $D=0$, which is removed by the Jacobian factor in the spherical coordinates.

The nonlocal correlation energy density can be approximated by the sum

$$\varepsilon_c^{\text{nl}}(\mathbf{r}) \approx \sum_{ij} \varphi(\mathbf{r}, \mathbf{r} + \tilde{\mathbf{r}}_{ij}) n(\mathbf{r} + \tilde{\mathbf{r}}_{ij}) w_{\text{rad}}(\tilde{r}_i) w_{\text{ang}}(\tilde{\Omega}_j), \quad (6)$$

where the weights $w_{\text{rad}}(\tilde{r}_i)$ and $w_{\text{ang}}(\tilde{\Omega}_j)$ correspond to the radial and angular parts of the integral, respectively. The latter is calculated on a Lebedev grid $\tilde{\Omega}_j$.¹³ The Gauss-Chebyshev quadrature of the second kind yields the radial integral weights $w_{\text{rad}}(\tilde{r}_i)$. The substitution,

$$\tilde{r} = r_m \sqrt{\frac{1-x}{1+x}}, \quad (7)$$

is used to map the initial integration range $0 < \tilde{r} < \infty$ to the range $-1 < x < 1$. The parameter r_m scales the grid and can be selected so that the quadrature grid $\tilde{\mathbf{r}}_{ij}$ adapts to the behavior of the kernel function. The kernel function experiences most rapid variations at small D values up to $D_{\text{max}} \approx 2$. This defines the range of \tilde{r} , where the contribution to the integral [Eq. (5)] is the largest and also the most difficult to calculate. If $r_m = 1/q_0(\mathbf{r})$, on average half of the grid points corresponds to $D < 1$ and $\sim 70\%$ to $D < 2$.

The above-described approach requires an algorithm to evaluate the density $n(\mathbf{r})$ and the wave number $q_0(\mathbf{r})$ at any point in the space. In many electronic-structure codes, the valence electron density is represented as a smooth function on a Cartesian grid, which is used also for representing the potential and integrating $\varepsilon_c^{\text{nl}}(\mathbf{r})$ to obtain E_c^{nl} . Trilinear or tricubic interpolation can be used to evaluate this function on the spherical quadrature grid on which the more rapidly varying kernel function can be represented accurately enough.

The explicit expression for $\varphi(\mathbf{r}, \mathbf{r}')$ involves a two-dimensional integral and is not suitable for practical calculations due to its complexity. Similarly to the previous approaches,^{4,11} we use a look-up table to evaluate

$D^2 \varphi(D, \Delta)$. The derivatives $\partial \varphi / \partial D$ and $\partial \varphi / \partial \Delta$ appearing in Eq. (4) are preferably evaluated from the same table instead of storing them separately as in Ref. 11. In the present work, this is done by bivariate cubic spline interpolation that allows us to obtain smooth first derivatives and is constructed by assuming continuous piecewise-bilinear second derivatives.

The order of computational complexity of evaluating $\varepsilon_c^{\text{nl}}(\mathbf{r})$ and $v_c^{\text{nl}}(\mathbf{r})$ at a given \mathbf{r} is $O(1)$ since the evaluation is limited by the size of the spherical coordinate grid $\tilde{\mathbf{r}}_{ij}$ and does not directly depend neither on the size of the Cartesian grid nor on the number of atoms N_{at} . Formally, the nonlocal correlation energy density and potential have to be calculated in all N_{grid} points of the Cartesian grid. For a sparse system, the volume of regions with zero or nearly zero electron density may be substantial. Calculating the nonlocal correlation energy density and potential at such points is very cheap, so it matters only how many Cartesian grid nodes with nonzero electron density there are. This number is proportional to the volume taken by the atoms, which in turn is roughly proportional to N_{at} and the density of the Cartesian grid points $1/v_{\text{grid}}$. Based on these considerations, the nonlocal correlation energy density and potential have to be evaluated in $O(N_{\text{at}} \cdot 1/v_{\text{grid}})$ points, which determines the order of the overall computational complexity.

The computational expense can be decreased without changing the order of complexity when additional adapting of both the radial and angular quadrature grids is done. Equation (1) implies that different regions of space do not contribute to E_c^{nl} equally, and thus it is not necessary to have quadratures with the same order of accuracy at every point. Low electron density regions can be treated by using radial grids \tilde{r}_i with less points than needed in grids at high-density regions. Moreover, the smoothness of the electron density can be used to reduce the sizes of angular grids Ω_j so that, when \tilde{r} decreases, less spherical harmonics are required to calculate the integral on the sphere.

We have implemented the vdW-DF into the SIESTA code.¹⁴ We use Troullier-Martins norm-conserving pseudopotentials generated with the Perdew-Burke-Ernzerhof (PBE) exchange-correlation functional.¹⁵ Sankey-type orbitals with the energy shift of 3 meV are used to generate the basis set on the triple zeta with polarization level.

In order to illustrate our adaptive-grid algorithm, we perform calculations for a Ne dimer. Figure 1 shows how the computational expense is distributed at different levels of optimization. The level of accuracy for evaluating the energy density $\varepsilon_c^{\text{nl}}(\mathbf{r})$ is the same in all these calculations. If the number of points in the quadrature grid $\tilde{\mathbf{r}}_{ij}$ is not varied [Fig. 1(a)], the evaluation of $\varepsilon_c^{\text{nl}}(\mathbf{r})$ is almost equally expensive in high- and low-density regions. If only the radial grid is adapted [Fig. 1(b)], the high-density regions are the most expensive to process and the total computational cost is clearly smaller than in the previous approach. Finally, when both radial and angular grids are adapted [Fig. 1(c)], there is a small island halfway between the Ne atoms and intermediate-density regions that require the largest effort.

Figure 1(d) shows the difference in the quantity $e_c^{\text{nl}}(\mathbf{r}) = n(\mathbf{r}) \varepsilon_c^{\text{nl}}(\mathbf{r})$ calculated between the dimer and the individual atoms. Remarkably, the island between the Ne atoms noticeably affects the bonding by adding a repulsive component to the interaction energy of the atoms.

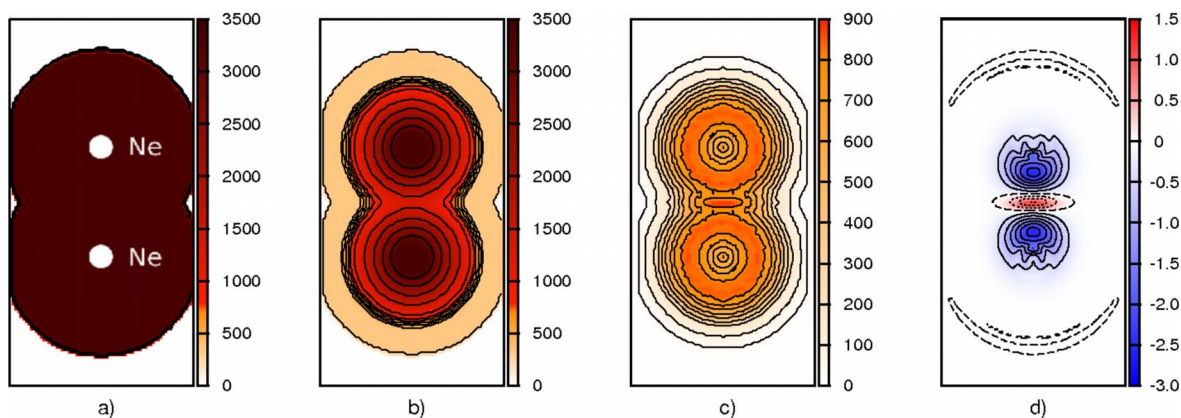


FIG. 1. (Color online) Test system of a Ne dimer. The positions of the nuclei with the distance of 3.0 Å are shown in part (a). (a)–(c) The distribution of sizes of quadrature grids used for the evaluation of $\epsilon_c^{nl}(\mathbf{r})$ and $v_c^{nl}(\mathbf{r})$ on different levels of adaptation is shown. (a) The quadrature grid size is not varied. (b) Only the number of radial shells is adjusted. (c) Both the radial and angular grids are adapted. (d) The nonlocal correlation energy contributions to the binding energy are shown. The plotted quantity is the difference in the function $10^5 \cdot n(\mathbf{r})\epsilon_c^{nl}(\mathbf{r})$ (in atomic units) between the dimer and the two free atoms at the dimer distance. The solid, long-, and short-dashed isolines correspond to negative, zero, and positive values, respectively.

In order to perform an extensive test of the vdW-DF and its present implementation, we have investigated the S22 set of molecules.¹² The structures of the molecules are completely optimized with the force convergence threshold of 0.01 eV/Å. The real-space grid cutoff of 250 Ry is chosen to diminish the “egg-box” effects due to the representation of the exchange-correlation potential on the Cartesian grid. When calculating the interaction energies, the basis set superposition error is estimated by using the counterpoise correction method.¹⁶ The typical size of the correction is 20 % of the total interaction energy.

The original approach by Dion *et al.*⁴ implies the use of the revised Perdew-Burke-Ernzerhof (revPBE) exchange.¹⁷ Such an approach is based on the notion that this exchange functional provides little or no bonding for van der Waals systems. On the other hand, it is known that revPBE systematically overestimates experimental bond lengths¹⁸ and gives smaller binding energies than the PBE or the Perdew-Wang 91 (Ref. 19) functional, which are more frequently used for different applications. Thus, it is important to understand the performance of the vdW-DF depending on the choice of the exchange functional. This has been addressed previously by Vydrov *et al.*²⁰ who found for a limited set of examples that the use of the revPBE exchange matches experimental or highly accurate quantum-chemical data better than the PBE or the exact exchange functional.

In the present Rapid Communication, we consider the revPBE and PBE exchange functionals. The results for the binding energies of the S22 molecular complexes are shown in Table I and visualized in Fig. 2. Table I shows a few systematic trends for the interaction energies obtained with different exchange functionals within the vdW-DF scheme. The complexes are bound stronger when employing the PBE than the revPBE exchange functional reflecting the more repulsive exchange interaction at the relevant intermolecular distance range when the latter functional is used. For the systems with predominant dispersion contributions and mixed complexes, as grouped in Table I, the revPBE exchange functional is somewhat more advantageous, as just-

TABLE I. Calculated binding energies (in meV) for the S22 model systems of Ref. 12. Complexes 1–7 are hydrogen bonded. Complexes 8–15 are with predominant dispersion interaction. The remaining ones are complexes with mixed bonding character.

Complex	vdW-DF		
	revPBE ^a	PBE ^a	CCSD(T) ^c
1 (NH ₃) ₂	106	161	137
2 (H ₂ O) ₂	177	242	218
3 Formic acid dimer	610	793	807
4 Formamide dimer	542	698	692
5 Uracil dimer	701	893	895
6 2-pyridoxine·2-aminopyridine	608	778	725
7 Adenine·thymine	586(659 ^b)	762	710
8 (CH ₄) ₂	38	67	23
9 (C ₂ H ₄) ₂	61	116	65
10 Benzene·CH ₄	60(68 ^b)	109	65
11 Benzene dimer (slip-parallel)	119(119 ^b)	215	118
12 Pyrazine dimer	168	271	192
13 Uracil dimer (stack)	356(305 ^b)	560	439
14 Indole·benzene (stack)	188	318	226
15 Adenine·thymine (stack)	425(414 ^b)	639	530
16 Ethene·ethine	67	103	66
17 Benzene·H ₂ O	118(118 ^b)	180	142
18 Benzene·NH ₃	81	138	102
19 Benzene·HCN	168	238	193
20 Benzene dimer (T-shape)	89	173	119
21 Indole·benzene (T-shape)	205	299	248
22 Phenol dimer	252	369	306

^aPresent Rapid Communication.

^bReference 7.

^cReference 12.

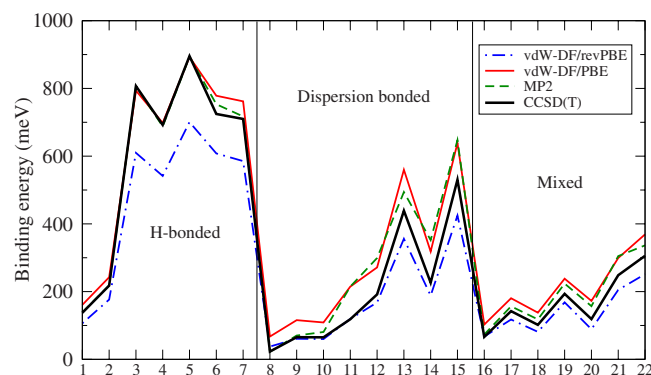


FIG. 2. (Color online) Binding energies for molecular complexes listed in Table I. The MP2 and CCSD(T) results are from Ref. 12.

fied by the good agreement with the CCSD(T) data.¹² On the other hand, the hydrogen-bonded complexes are poorly described if the revPBE exchange is used with the vdW-DF, while the results obtained with the PBE exchange functional match well the reference data.

Some of the S22 systems have been studied earlier by Cooper *et al.*⁷ using revPBE exchange. However, they did not optimize the geometries completely but relied on a partial relaxation. Moreover, in the present work, basis functions

and pseudopotentials differ from the previous ones, and also therefore one cannot expect a perfect matching with the earlier results. Nevertheless, as shown in Table I the binding energies are in rather good agreement with the exception of the hydrogen-bonded adenine-thymine complex for which the difference is 74 meV.

In conclusion, we have demonstrated an efficient real-space algorithm to evaluate the vdW correlation energy and potential. The application to the noncovalently bound complexes of the S22 set reveals a remarkable agreement between the vdW-DF and accurate quantum chemistry methods. The dependence on the exchange functional used with vdW-DF has been confirmed. While it has been believed that the revPBE exchange functional is the most appropriate one for vdW-DF calculations, we have shown a class of counterexamples demonstrating a systematic underbinding when using the revPBE, while the PBE exchange functional succeeds well. Such observations imply that none of the popular GGA exchange functionals can be considered as universal for problems where noncovalent bonds play the major role.

This research has been supported by the Academy of Finland through its Centers of Excellence Program (2006-11). We are also grateful to Bengt Lundqvist and David Langreth for useful discussions.

- ¹F. Jensen, *Introduction to Computational Chemistry* (John Wiley & Sons, New York, 1998).
- ²C. Pisani, L. Maschio, S. Casassa, M. Halo, M. Schuetz, and D. Usvyat, *J. Comput. Chem.* **29**, 2113 (2008).
- ³B. Paulus, *Phys. Rep.* **428**, 1 (2006).
- ⁴M. Dion, H. Rydberg, E. Schröder, D. C. Langreth, and B. I. Lundqvist, *Phys. Rev. Lett.* **92**, 246401 (2004).
- ⁵D. C. Langreth, M. Dion, H. Rydberg, E. Schröder, P. Hyldgaard, and B. I. Lundqvist, *Int. J. Quantum Chem.* **101**, 599 (2005).
- ⁶D. C. Langreth *et al.*, *J. Phys.: Condens. Matter* **21**, 084203 (2009).
- ⁷V. R. Cooper, T. Thonhauser, and D. C. Langreth, *J. Chem. Phys.* **128**, 204102 (2008).
- ⁸K. Johnston, J. Kleis, B. I. Lundqvist, and R. M. Nieminen, *Phys. Rev. B* **77**, 121404(R) (2008).
- ⁹S. D. Chakarova-Käck, E. Schröder, B. I. Lundqvist, and D. C. Langreth, *Phys. Rev. Lett.* **96**, 146107 (2006).
- ¹⁰P. Sony, P. Puschnig, D. Nabok, and C. Ambrosch-Draxl, *Phys. Rev. Lett.* **99**, 176401 (2007).
- ¹¹T. Thonhauser, V. R. Cooper, S. Li, A. Puzder, P. Hyldgaard, and D. C. Langreth, *Phys. Rev. B* **76**, 125112 (2007).
- ¹²P. Jurečka, J. Šponer, J. Černý, and P. Hobza, *Phys. Chem. Chem. Phys.* **8**, 1985 (2006).
- ¹³V. I. Lebedev, *Zh. Vychisl. Mat. Mat. Fiz.* **15**, 48 (1975).
- ¹⁴P. Ordejón, E. Artacho, and J. M. Soler, *Phys. Rev. B* **53**, R10441 (1996).
- ¹⁵J. P. Perdew, K. Burke, and M. Ernzerhof, *Phys. Rev. Lett.* **77**, 3865 (1996).
- ¹⁶S. F. Boys and F. Bernardi, *Mol. Phys.* **19**, 553 (1970).
- ¹⁷Y. Zhang and W. Yang, *Phys. Rev. Lett.* **80**, 890 (1998).
- ¹⁸J. P. Perdew, K. Burke, and M. Ernzerhof, *Phys. Rev. Lett.* **80**, 891 (1998).
- ¹⁹J. P. Perdew, J. A. Chevary, S. H. Vosko, K. A. Jackson, M. R. Pederson, D. J. Singh, and C. Fiolhais, *Phys. Rev. B* **46**, 6671 (1992).
- ²⁰O. A. Vydrov, Q. Wu, and T. V. Voorhis, *J. Chem. Phys.* **129**, 014106 (2008).